

Thermal Diffusivity Measurements of $Zn_{1-x-y}Be_xMn_ySe$ Mixed Crystals by Photoacoustic Method

J. Zakrzewski, F. Firszt, S. Łęgowski, H. Męczyńska, M. Pawlak

Institute of Physics, Nicolas Copernicus University, ul.Grudziądzka 5/7, 87-100 Toruń, Poland

Diluted magnetic semiconductors obtained by alloying II-VI compounds with manganese chalcogenides recently received great attention for their potential application in magnetoelectronics [1]. However to date, there is little published data on quaternary diluted magnetic semiconductors thin layers [2] and no on bulk crystals. This paper deals with photoacoustic (PA) study of $Zn_{1-x-y}Be_xMn_ySe$ ($0 < x < 0.25$, $0 < y < 0.50$) solid solutions.

The investigated crystals were grown from the melt by the modified high pressure Bridgman technique under argon overpressure (13.5 MPa) as described in [3]. Their compositions were determined by wet chemical analysis. All

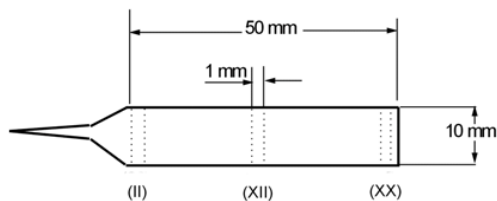


Fig. 1. The shape and dimensions of $Zn_{1-x-y}Be_xMn_ySe$ mixed crystal. Samples cut from the bulk crystal are indicated

samples used in this experiment were as grown. Photoacoustic (PA) measurements were carried out using an open cell. The xenon lamp and He-Cd laser (325 nm) were used as excitation sources for PA spectra and thermal diffusivity measurements, respectively. PZT transducer and lock-in amplifier (Stanford SR-510) were applied for detection of PA signal using wave conversion method.

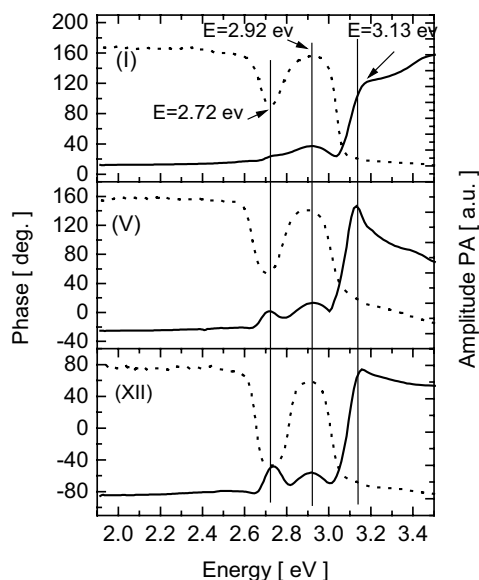


Fig. 2. Photoacoustic phase (dot) and amplitude (solid) of $Zn_{0.73}Be_{0.25}Mn_{0.02}Se$ for modulation frequency 36 Hz

The shape and dimensions of crystals obtained are given in figure 1. The crystals were cut into 1-1.5 mm thick plates, mechanically polished and chemically etched. There were measured samples from seven bulk crystals with the different Mn and Be contents. The change of Mn and Be content with distance from the top of the bulk was expected. However for the three samples, cut from the different places, shown in figure 2 there is almost no change of the structure of the spectra. For each sample two maxima ($E = 2.72 \text{ eV}$ and $E = 2.92 \text{ eV}$) of the PA amplitude spectra in sub-band-gap region are observed. A maximum at $E = 2.72 \text{ eV}$ is observed in phase spectra as well. For sample (I) an increase of PA amplitude and for samples (V) and (XII) decrease of PA amplitude are observed, respectively. This could be due to the presence of inhomogeneity of the sub-surface layer.

Further measurements were carried out only for one sample from each series.

Fig 3 shows photoacoustic spectra of $Zn_{1-x-y}Be_xMn_ySe$ measured at room temperature for modulation frequency 6 Hz. It can be seen that the shift of fundamental edge towards higher

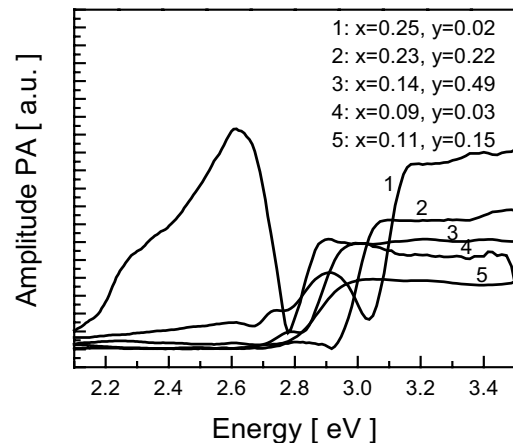


Fig. 3. Photoacoustic spectra of $Zn_{1-x-y}Be_xMn_ySe$ mixed crystals for different Be and Mn content for modulation frequency 6 Hz

energies is observed for different compositions. The Jackson-Amer [4] model of the piezoelectrically detected PA effect was applied to analyze obtained spectra. The estimated values of energy gap are shown in Table 1.

For the $Zn_{0.73}Be_{0.25}Mn_{0.02}Se$ and $Zn_{0.88}Be_{0.09}Mn_{0.03}Se$ samples PA spectra exhibit structures in the sub-band-gap region. (Fig. 4). The position of the amplitude signal maximum for the $Zn_{0.73}Be_{0.25}Mn_{0.02}Se$ mixed crystals shifts towards higher energy with increasing modulation frequency and the intensity of the peak decreases. No change of the phase signal is observed in that region. The position of two maxima in sub-band-gap region observed in the spectra of $Zn_{0.88}Be_{0.09}Mn_{0.03}Se$ do not change with the increase of modulation frequency. The changes of phase are observed for the same energy values. The behavior of these two samples shows that the origin of the photoacoustic signal should be different. The PA signal in the sub-band-gap

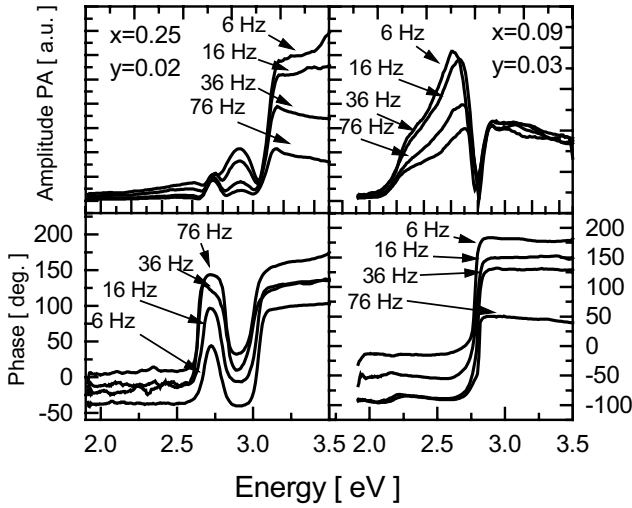


Fig.4. Amplitude and phase of photoacoustic signal of $Zn_{0.73}Be_{0.25}Mn_{0.02}Se$ and $Zn_{0.88}Be_{0.09}Mn_{0.03}Se$ mixed crystals for different modulation frequencies

region and the energy shift of maximum in the presence of an applied electric field was observed for CdS by Mandelis and Siu [5]. In our experiments the electrical arrangement of the cell described by M. Watanabe [6] was applied. When the photoacoustic signal was collected from the electrode situated between the sample and detector, additional surface photovoltage was observed. It can result in the raise of signal due to Joule effect. This effect is obviously enhanced in fractured samples or the ones with the high defect concentrations. For $Zn_{0.88}Be_{0.09}Mn_{0.03}Se$ mixed crystal the changes of phase show the change of oscillation modes of the sample due to the presence of localized states in sub-band gap region.

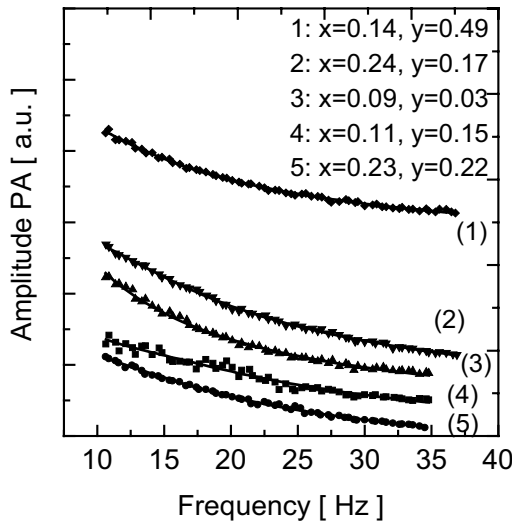


Fig. 5. Amplitude of PA signal as a function of modulation frequency for $Zn_{1-x-y}Be_xMn_ySe$

Another very important physical parameter – thermal diffusivity, which characterizes the time required to establish the thermal equilibrium in semiconductors and is strongly sensitive to the structure properties, was also determined. The

model developed by Blonskij et. al. [7] was applied. They averaged the thermal diffusion equations over the area of the sample and solved the thermoelastic problem. The analytical expressions for the amplitude and phase for opaque sample were derived, namely:

$$|V| = \frac{P\alpha}{kla^2} \psi(al),$$

$$\psi(al) = \left\{ \left[1 - \frac{3 \sinh(al) + \sin(al)}{2al \cosh(al) + \cos(al)} \right]^2 + \left[\frac{3 \sinh(al) - \sin(al)}{2al \cosh(al) + \cos(al)} \right]^2 \right\}^{1/2}$$

$$\tan \varphi = \frac{\frac{3 \sinh(al) - \sin(al)}{2al \cosh(al) + \cos(al)}}{1 - \frac{3 \sinh(al) + \sin(al)}{2al \cosh(al) + \cos(al)}}$$

where V, φ are signal amplitude and phase, respectively, α - absorption coefficient, k - thermal conductivity, l - sample thickness, P - constant, $a = \sqrt{\omega/2D}$, $\omega = 2\pi f$, f - modulation frequency, D - thermal diffusivity.

Fig. 5 presents the PA signal amplitude as a function of modulation frequency for $Zn_{1-x-y}Be_xMn_ySe$ crystals with different Be content (laser excitation). The solids lines represent the best fit to experimental data according to Blonskij's et. al. expressions.

The estimated values of thermal diffusivity at 300 K of $Zn_{1-x-y}Be_xMn_ySe$ mixed crystals derived from the analysis of frequency dependence of PA signal are presented in Table 1.

Be	Mn	Thermal diffusivity [cm ² /s]	E _g [eV]
0.09	0.03	0.030±0.016	2.89±0.02
0.14	0.49	0.096±0.015	2.94±0.02
0.11	0.15	0.133±0.035	2.97±0.02
0.23	0.22	0.084±0.012	3.03±0.02
0.24	0.17	0.123±0.013	3.06±0.02
0.25	0.02	0.133±0.038	3.15±0.02

Table 1. The values of thermal diffusivities and energy gaps of $Zn_{1-x-y}Be_xMn_ySe$ mixed crystals for different Be and Mn content

- [1] R. FITZGERALD, *Physic Today* **21**, April (2000)
- [2] R. FIEDERLING, M. KEIN, G. REUSCHER, W. OSSAU, G. SCHMIDT, A. WAAG, L. W. MOLENKANYO, *Nature* **402**, 787 (1999)
- [3] W. PASZKOWICZ, K. GODWOD, J. DOMAGAŁA, F. FIRSZT, J. SZATKOWSKI, H. MĘCZYŃSKA, S. ŁĘGOWSKI and M. MARCZAK, *Solid State Commun.* **107**, 735, (1998)
- [4] J. W. JACKSON, N. M. AMER, *J. Appl. Phys.*, **51**, 3343 (1980)
- [5] A. MANDELIS, E. K. M. SIU *Phys. Rev B*, **34**, 7209 (1986).
- [6] M. WATANABE in „Photoacoustic and Photothermal Phenomena” eds. P. Hess, J. Pelzl, Springer-Verlag, 254, (1988)
- [7] I. V. BLONSKIJ, V. A. THORYK, M. L. SHENDELEVA, *J. Appl. Phys.*, **79**, 3512 (1996).